AIAA 81-2021R

Tests of a Thermal Acoustic Shield with a Supersonic Jet

N. Pickup,* R.A. Mangiarotty,† and J.V. O'Keefe‡
The Boeing Company, Seattle, Washington

A thermal acoustic shield on a scale-model, high-radius-ratio plug nozzle has been static tested at nozzle pressure ratios up to 4.5, with shield velocity ratios of 0.4-0.7, at two nominal thicknesses. Shield flow rates and acoustic attenuation were less than expected due to the interaction of the primary nozzle flow, which effectively reduced the shield thickness. Noise reduction due to shielding improves up to a pressure ratio of 3.0 and diminishes at greater ratios for the configuration tested. There appears to be some reduction in shock-cell noise up to 3.5 pressure ratio, with amplification at greater pressure ratios. Absolute jet temperature (as opposed to temperature ratio) appears to be significant to noise reduction at the higher jet velocities. It is concluded that a thermal acoustic shield has great potential, but that the acoustic benefit is implementation-dependent and, consequently, that obtaining the greatest benefits of the shield will be a challenge to designers.

Nomenclature

ADP-1 = acoustic data processor (computer) system 1
con-di = convergent-divergent (nozzle)
dB = decibels = $20 \log_{10}(P_0/P_{ref})$
EPNL = effective perceived noise level
EPNdB = effective perceived noise, dB (EPNL units)
M_j = jet Mach number
PNdB = perceived noise, dB (PNL units)
PNL = perceived noise level
PNLW = an angle weighting of PNL to estimate the effectiveness of a suppression device on an airplane flyover =

$$10 \log_{10} \sum_{\theta=60\,\text{deg}}^{160\,\text{deg}} 10^{\left[\frac{\text{PNL}(\theta) - 10 \log_{10} \sin^2\theta}{10}\right]}$$

PR = pressure ratio
radius ratio = nozzle inner radius (r_i)/nozzle outer radius (r_o)
RC = round convergent (nozzle)
SPL = sound pressure level
TAS = thermal acoustic shield
T_T = total temperature
V_j = jet velocity (ideal)

Introduction

THIS paper is concerned with scale-model static tests of one particular concept for achieving jet noise reduction, the thermal acoustic shield (TAS) (also known as "hot-gas shield" and/or "fluid dynamic shield"). Other suppression devices being considered for SST application are the coannular nozzle, internally ventilated nozzle, and mechanical suppressors.

The application of the TAS to an SST is illustrated in Fig. 1. In this concept, the shield gas is bled from the primary jet through choke plates (to reduce the velocity) into a 180 deg semiannular jet. This semiannular jet reflects and refracts noise from the primary jet,[1-3] reduces shear, and gives pressure field interactions that affect shock-cell noise. Note that since the shield jet is obtained by bleed, this source is at the same total temperature as the primary jet.

In addition to the open literature (e.g., Refs. 1-4), an extensive test data base also has been accumulated through various application studies at Boeing. This work resulted in the assessment of major TAS controlling parameters given in Table 1. This data base, as well as the work of others, does not extend to the high jet velocities applicable to the SST nor does it include the TAS used in combination with a high-radius-ratio plug nozzle, as it would for an SST engine. A test program was therefore initiated to determine acoustic performance of the configuration.

Test Description

The tests were performed in the Boeing Large Test Chamber (LTC) using facilities described in Ref. 5. The tests were run at static conditions for proof of concept/screening purposes only. Test models are generic in design and are not intended to be a precise representation of a specific exhaust system. Since the variable-area nozzle was represented by fixed-area models, correspondence is obtained by using variable-scale factors in data reduction and analysis.

Model Configurations

The test configurations, with the appropriate test conditions, are given in Table 2.

The RC (or conic) baseline, configuration 1, nozzle exit diameter is 4.6 in. with a cold-flow throat area of 16.6 in.^{2}. Configuration 2 was the TAS model with the secondary (shield) nozzle assembly removed. The nozzle radius ratio (r_o/r_i) as tested was 0.85, with a cold-throat area of 14.9 in.^{2} and a scale factor of one-eighth at the highest throttle setting. The tested nozzle termination form was convergent (conic).

The TAS model shown in Fig. 2 has the shield nozzle formed by a duct bifurcation that diverts the secondary nozzle flow into a 180 deg arc. Previous Boeing tests had shown that a simple blanking plate gave severely distorted shield flows (of uneven thickness). To avoid this vena-contracta effect, the bifurcation was designed to give a smooth transition from a full annulus to the 180 deg arc with an adequate straightening section at the exit. The two different shield thicknesses, configurations 3 and 4, were achieved by two different nozzle lips, as indicated in Fig. 2. The shields were designed to give geometric full-scale thicknesses of 6 and 12 in. for the thin and thick shields, respectively. The effective thickness based on measured airflow and exit velocities was different from the geometric thickness and will be discussed later.

Presented as Paper 81-2021 at the AIAA 7th Aeroacoustics Conference, Palo Alto, Calif., Oct. 5-7, 1981; submitted Oct. 13, 1981; revision received Feb. 8, 1982.

*Specialist Engineer.
†Principal Engineer.
‡Unit Chief, Noise Technology Staff NP/PD. Associate Fellow AIAA.

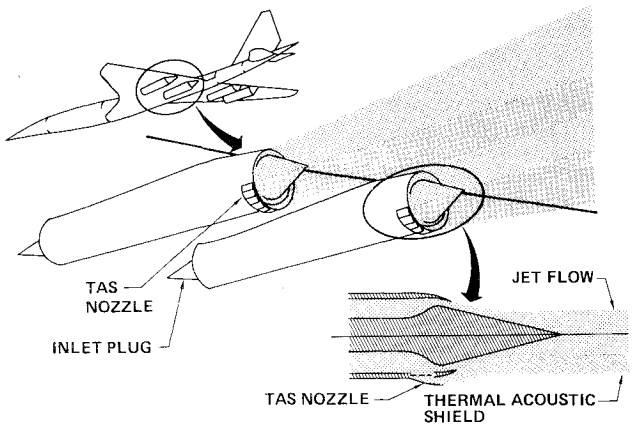

Fig. 1 Application of thermal acoustic shield (engine bleed system type).

Table 1 TAS controlling parameters

Shield thickness h, in.
Range tested: $0.06 < h/D < 0.45$ (1.7-13 in., full scale)
Optimum: no definable optimum—thicker→better
Shield temperature t, °F
Range tested: $0.05 < t/T < 8.4$ (65-1000-3000°F simulated)
Optimum: no definable optimum—hotter→better
Shield velocity v, ft/s
Range tested: $0.1 < v/V < 0.7$ (160-1100 ft/s)
Optimum: generally $v/V < 0.5$, but varies with nozzle, temperature, and thickness
Shield angle θ, deg
Range tested: 180-240 and 360 deg
Optimum: 240 deg (for sideline)
Gap ψ, in.
Range tested: zero to large (not parametrized)
Optimum: application dependent

The geometry of the configuration 2-4 nozzles is shown in Table 3.

Test Jet Conditions

The nominal primary jet test conditions are given in Table 2. This approximates a typical SST throttle line up to the 3.5 pressure ratio. The full-size engine line extends to 4.5 pressure ratio and 2200°R. The test line represented the limit to which the test facility would permit the engine line to be followed. Thus, while the engine can operate with jet velocities up to 3000 ft/s (dependent on size), test data are limited to 2600 ft/s (even less for shield fully mixed velocities). Followup tests to expand the data base extended the pressure ratio to 4.5, but limited temperature in these cases to 1560°R (and consequently jet velocity to less than 2600 ft/s).

For these tests, the shield jet was provided by a separate source that could be independently controlled with the shield temperature set the same as for the primary jet. Test conditions for TAS were obtained by setting the shield jet pressure ratio to give the desired velocity ratio. The follow-on tests also included a 0.4 velocity ratio.

Instrumentation

Since the test program was primarily a proof of concept and screening, instrumentation was kept simple with only a single sideline array of microphones being used. The microphone layout shown in Fig. 3 had 10 microphones on a 15 ft sideline, with an 11th (the 60 deg one) on a 10 ft sideline. The 11 microphones covered an arc from 60 to 160 deg, relative to an engine inlet, in 10 deg intervals.

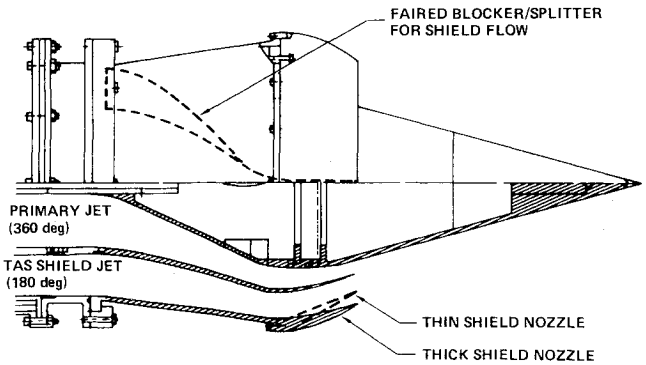

Fig. 2 Test model.

Table 2 Test conditions[a]

Configuration No.	Description	Test conditions (nominal)	
		V_j, ft/s	T_T, °R
1	Baseline conic	1500	1250
2	Baseline plug (radius ratio 0.85)	1800	1350
3	Plug with thin shield on centerline axis	2000	1500
		2400	1700
		2600	1850
4	Plug with thick shield on centerline axis	Velocity ratio 0.5, 0.6, 0.7	

[a] Test conditions apply to all configurations.

Table 3 Geometry of configuration 2-4 nozzles

	Primary (plug)	Thin shield	Thick shield
Mean nozzle diameter, in.	8.4	9.8	11.25
Mean throat gap, in.	0.606	0.660	1.331
Net cold-nozzle area, in.^{2}	14.9	9.6	20.9

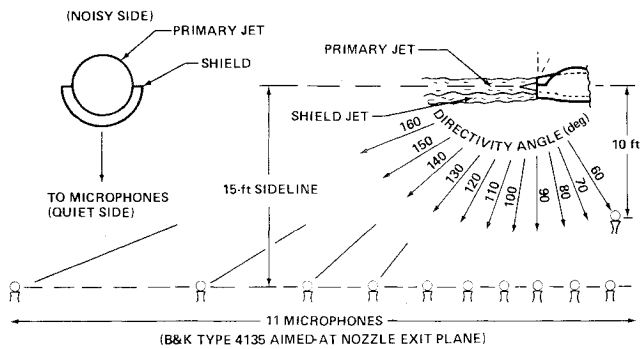

Fig. 3 Microphone layout.

In addition to the normal data channels, a Spectral Dynamics SD345 spectrum analyzer was set up to monitor the 90 deg microphone channel. This provided an online narrowband view of the noise in real time. This was to monitor shock-cell noise.

Test Results

In the work reported here the only "normalization" performed is that for atmospheric propagation at 77°F, 70% relative humidity, together with scaling as required. Jet velocities are the ideal velocities, as deduced from the

measured jet pressure and temperature aerothermal data.

In all cases where results are presented at different scales, they are obtained by scaling the as-measured data, which insures that comparisons are based on correct spectral content. Scaling is based on the assumption that model and full-size operating points are at identical pressure ratio and total temperature. Then weight flow scaling can be used since, with such equality, weight flow is a direct function of nozzle size.

There can be an error when scaling to an engine having a variable-area nozzle from a fixed-area model due to the engine plug nozzle having a varying radius ratio, whereas the model has a fixed one. For this test the error is expected to be zero at low velocity when the nozzle is open, and up to +1.3 dB at higher jet velocities when the nozzle is closed (higher radius ratio).

Shield Thickness Effects

Prior to the tests, an attempt was made to predict the results using the available data base. When the thin shield results were compared with these predictions, the results were disappointing. The thick shield results were in an acceptable range for the thin shield.

It was noted that the shield nozzle discharge coefficients were abnormally low, suggesting flowfield effects of the type given in Ref. 6, whereby primary nozzle flow has a back-pressure effect on the shield nozzle causing reduced flow. A subsequent analysis[7] substantiated the hypothesis.

Effective shield thickness was based on the fully expanded jet area obtained from values available in the test aerothermal data. Values of effective shield were calculated for each power setting and scaled to a nominal 640 lb/s engine as shown in Fig. 4. This effective thickness makes the measured noise suppression much more consistent with previous test results.

Spectrum Analysis

Noise spectra and directivity are shown in Figs. 5-11 plotted to an equal full-scale primary jet. This gives a true noise suppression result, but does not show any implementation-dependent characteristics, which are shown later in the PNLW data results. Only sample plots to show general characteristics for a 0.5 velocity ratio TAS on a 150 ft polar arc are given.

In several of the high-angle (e.g., 140 deg) spectra, there is an increase in noise with increasing frequency, an effect also noted in other literature.[4] This "tail-up" effect is believed to be spurious and is an area needing further investigation.

Figure 5 shows spectra for a thick shield with a just-supersonic jet (PR = 2.16, $T_T = 1370°R$, $V_j = 1800$ ft/s, $M_j = 1.11$). It can be seen that the high-radius-ratio plug nozzle substantially removes shock-cell noise, as well as giving mixing noise reduction. The TAS provides substantially higher frequency noise reduction at high angles. It also provides significant reduction at 90 deg and at forward (low) angles. The PNL directivity is given in Fig. 6. This shows that the greatest reduction with the plug baseline is for the forward, low angles, whereas TAS reduction is greater at the high angles. Relative to the conic baseline the thick TAS at this condition is a "13 peak PNdB suppressor" by definitions frequently used for suppressors.

At higher jet velocities, characteristics are generally similar to those at the lower velocity. Shock-cell noise is more pronounced, with the TAS apparently giving some additional reduction to this noise relative to the plug nozzle. The increase in very low-frequency noise due to the TAS is more apparent. In addition to reducing shock-cell noise, the TAS appears to shift the peak frequency by a small amount, which implies a

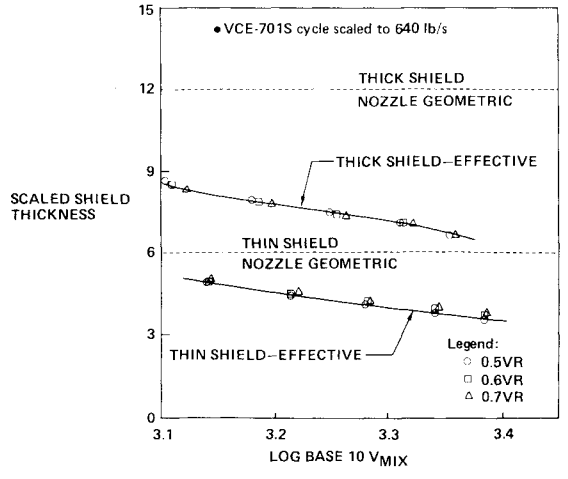

Fig. 4 Effective shield thickness.

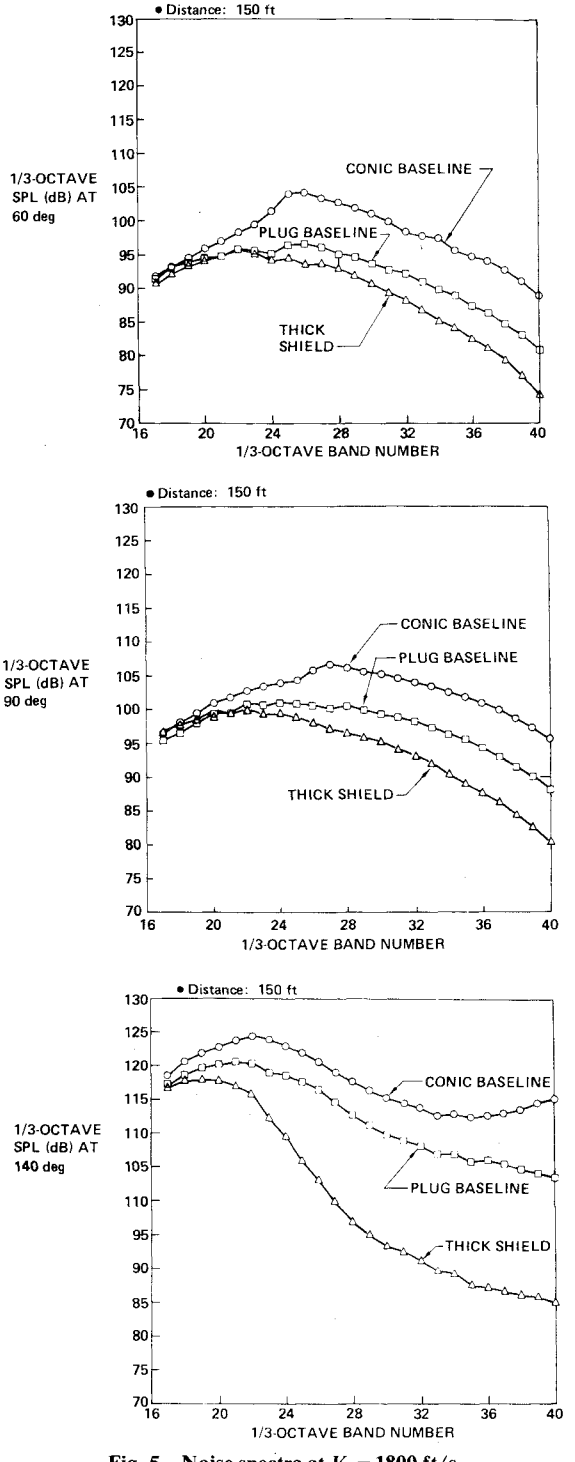

Fig. 5 Noise spectra at $V_j = 1800$ ft/s.

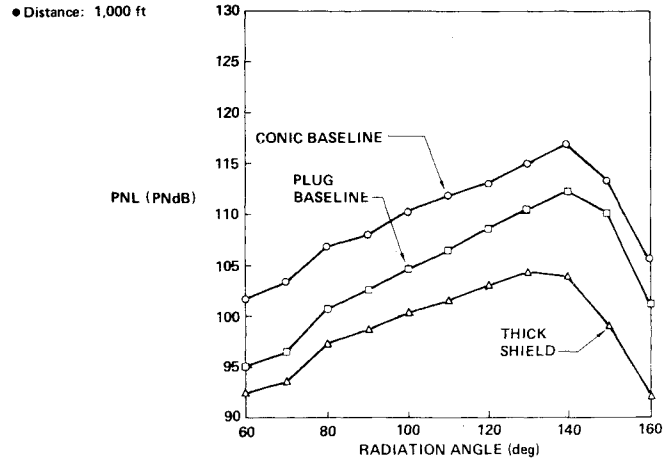

Fig. 6 PNL directivity at $V_j = 1800$ ft/s.

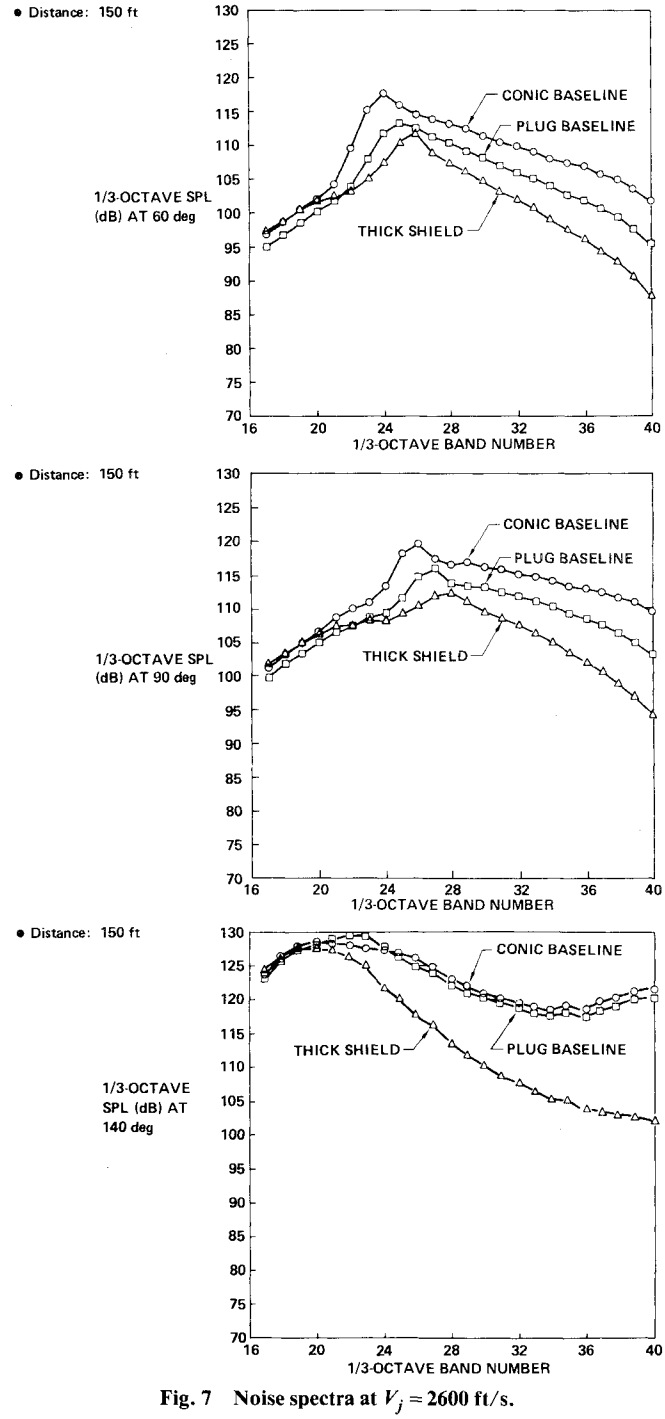

Fig. 7 Noise spectra at $V_j = 2600$ ft/s.

jet modifying effect. The directivity is similar to that of Fig. 6, but with reduced suppression (10 peak PNdB).

Spectra for the highest tested jet velocity spectra are given in Fig. 7 (PR = 3.5, $T_T = 1860°$R, $V_j = 2600$ ft/s, $M_j = 1.47$). Here, while the amount of reduction in shock-cell noise decreases, the TAS is still showing some modification effect. Mixing noise reduction is also significantly reduced, the plug baseline showing no advantage relative to the RC baseline at the high angles, as shown in Fig. 8.

The thin shield results show similar general characteristics except for the reduced level of suppression.

Results from a follow-on test show a further modification to shock-cell noise behavior at higher nozzle pressure ratios (to 4.5 at 1560°R). At PR = 4.0, $T_T = 1560°$R, $V_j = 2500$ ft/s, and $M_j = 1.57$, shock-cell noise for the plug baseline was reduced (Fig. 9), probably due to the formation of a Mach disk. The TAS noise however continues to increase, so that in the shock-cell noise dominated angles it becomes noisier than the plug baseline (Fig. 10). The TAS remains quieter than the plug baseline in the mixing-noise-dominated higher angles. Both plug baseline and TAS shock-cell noise spectra (60 deg) show a broader "haystack" to the shock-cell noise peak than at lower jet pressure ratios. The shock-cell TAS interactions are deserving of further, deeper study.

PNLW Analysis

The TAS is unique among suppression devices because of the high degree of dependence on the implementation method (Fig. 11).

As tested, the primary nozzles for the plug baseline and for the TAS are identical and are operated at identical conditions so that the two primary jets represent an equal noise source. Addition of the TAS gives a substantial noise reduction at the microphones, which in the example is 7.3 ΔPNLWdB. This ignores the propulsive system effects of the TAS and is the condition for the spectra analysis shown earlier.

As tested, the TAS adds substantially to the thrust of the system, by approximately 50%. If compared on an equal, as-tested, thrust basis, noise reduction is 12.4 ΔPNLWdB. This would be representative of the suppression that might be obtained if the TAS could be implemented in an additive form.

A practical form of implementation of the TAS is to obtain the shield jet by a bleed from the primary jet (Fig. 1). For example, taking 30% of total mass flow and reducing its velocity by a half results in a 15% thrust loss. This is illustrated in Fig. 11 by calculating thrust based on the primary jet weight flow only, but with a fully mixed jet velocity. This is not a precise representation since it treats the shielded case as having the same noise source as the unshielded, whereas the act of bleeding will also change the noise source (to a smaller jet). This simplification does however illustrate the loss in shield effectiveness due to thrust loss (4.8 ΔPNLWdB in the example of Fig. 11). In Figs. 12 and 13 the measured data have been scaled to a nominal 640 lb/s size engine. By scaling the data to include the effects of shield bleed, a more precise representation of the noise is obtained.

The resultant data, when scaled and normalized, give noise at equal thrust (equal jet velocity, equal weight flow). PNLW values are plotted in Fig. 12 and the 0.5 velocity ratio thick shield with delta PNLW values in Fig. 13. To obtain the Δ PNLW for the TAS relative to the RC baseline, add the plug and shield delta values in Fig. 13.

The highest measured TAS fully mixed jet velocity is 2255 ft/s (log = 3.353) for the thick shield and 2420 ft/s (log = 3.384) for the thin shield; thus the analytic results for jet velocities greater than these are extrapolated. The measured RC and plug baselines both show decreasing noise vs jet velocity slopes at the higher jet velocities. The TAS cases, on the other hand, show increasing slopes in the extrapolated region. The worst case expected result would be one asymptotic to the measured RC baseline, which the ex-

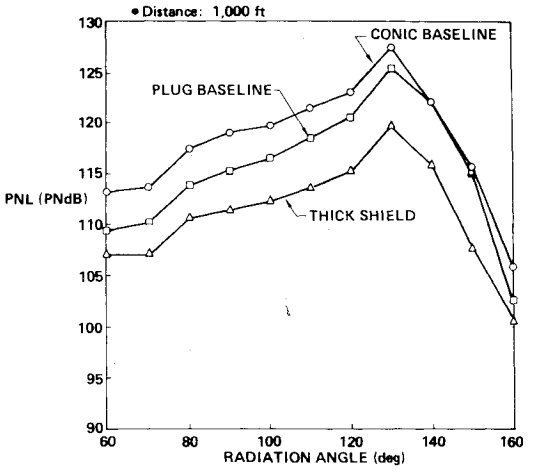

Fig. 8 PNL directivity at $V_j = 2600$ ft/s.

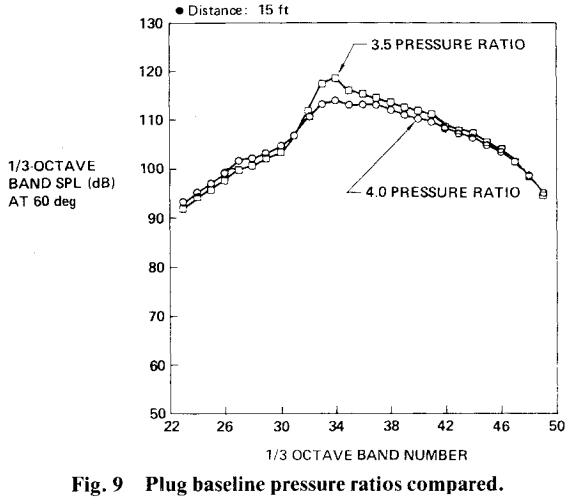

Fig. 9 Plug baseline pressure ratios compared.

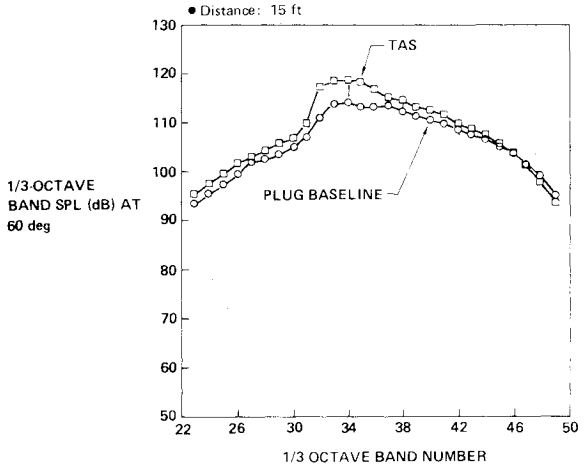

Fig. 10 TAS at 4.0 pressure ratio (shock-cell noise).

trapolation does not show. The fixed-scale results plotted in Figs. 14 and 15 are based on primary jet velocities and hence do not require extrapolation. These latter results show suppression, disregarding any propulsive effect of the shield.

Absolute Temperature Dependence

The follow-on test program to extend the data base was intended to investigate higher jet velocities by testing at pressure ratios up to 4.5. Test model/rig interface limitations, however, made it necessary to restrict the temperature to 1100°F at the high-pressure ratio. This meant that the test

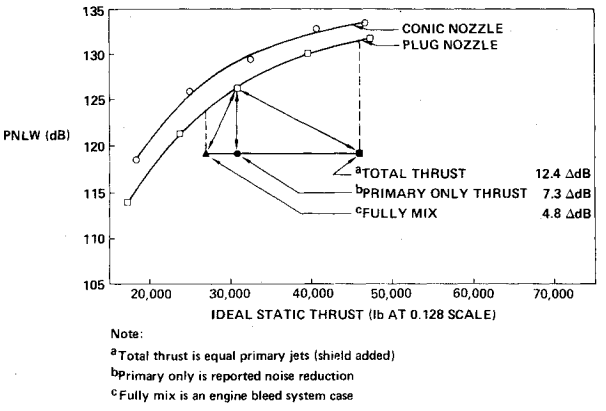

Fig. 11 Noise reduction evaluation.

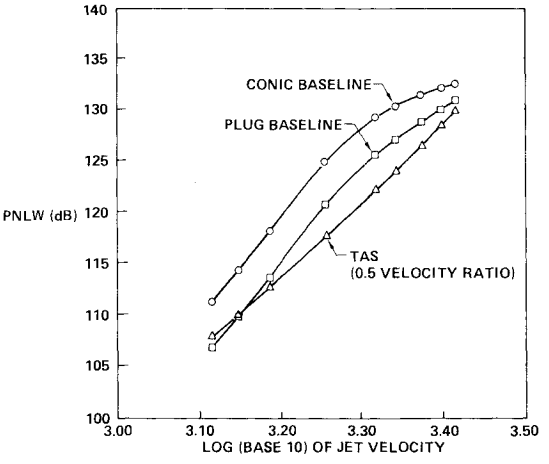

Fig. 12 Bleed system implementation scaling.

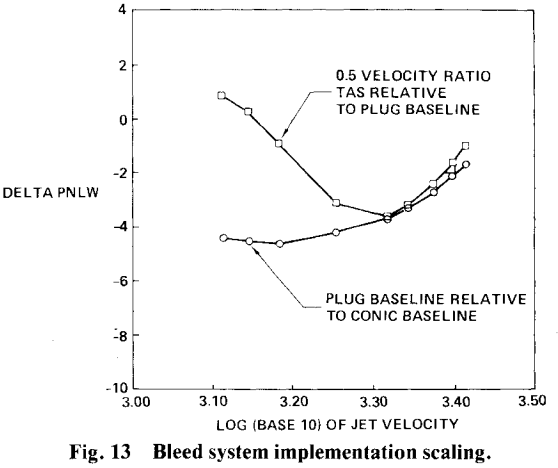

Fig. 13 Bleed system implementation scaling.

covered the same jet velocity (and hence normalized thrust) range as the earlier test. The shock-cell/mixing source noise balance would change, however.

It was found that results for the follow-on test, when compared with the earlier test on the basis of jet velocity (primary, mixed, or normalized thrust), showed substantially less noise suppression. This was unexpected since temperature ratios, velocity ratios, and other key parameters were the same for the two tests. Essentially, the only difference was absolute temperature. While comparing spectra at equal pressure ratios from the two tests to isolate the cause, it was found that there was no difference—tests at the same ratio with the TAS gave the same results (within a fraction of a dB). When the results of the two test series are plotted against pressure ratio (Fig. 16), they follow the same trend curve.

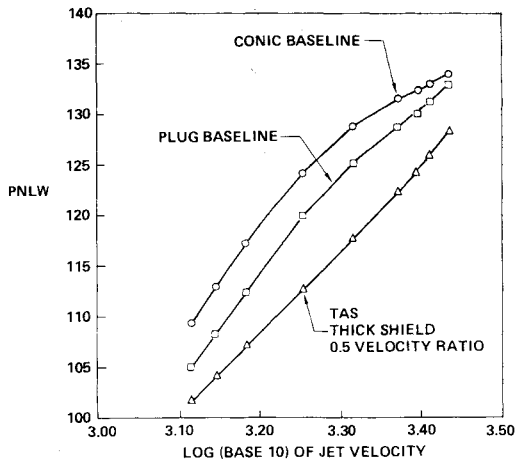

Fig. 14 Equal primary (shield added) fixed scaling.

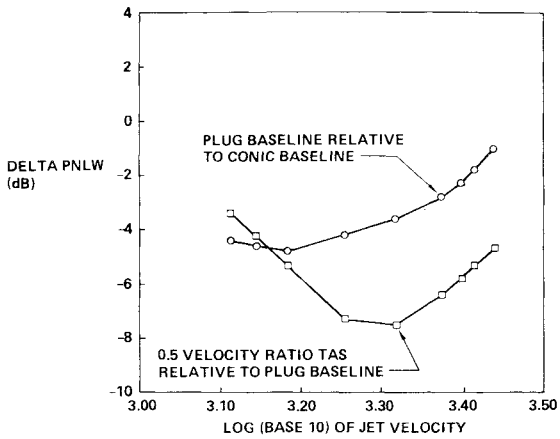

Fig. 15 Equal primary (shield added) fixed scaling.

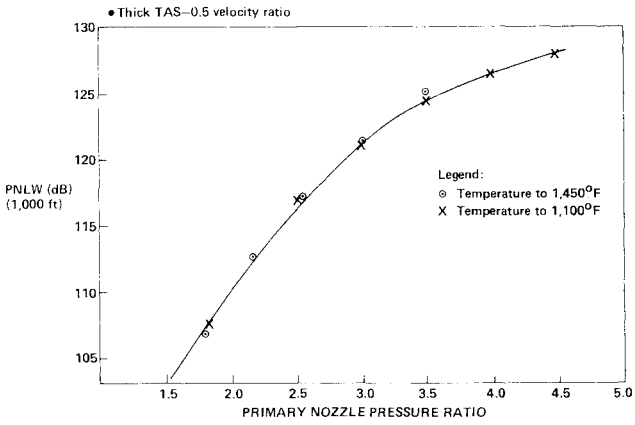

Fig. 16 Thermal acoustic shield tests compared.

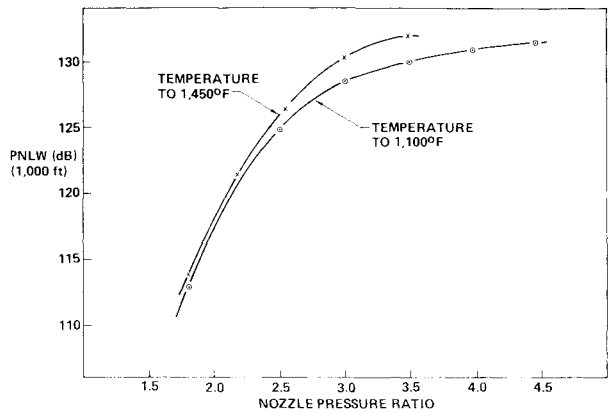

Fig. 17 Plug nozzle tests compared.

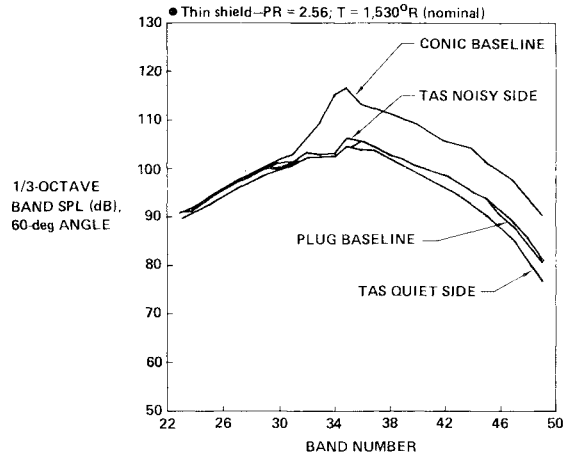

Fig. 18 Noisy-quiet side comparison, 60 deg.

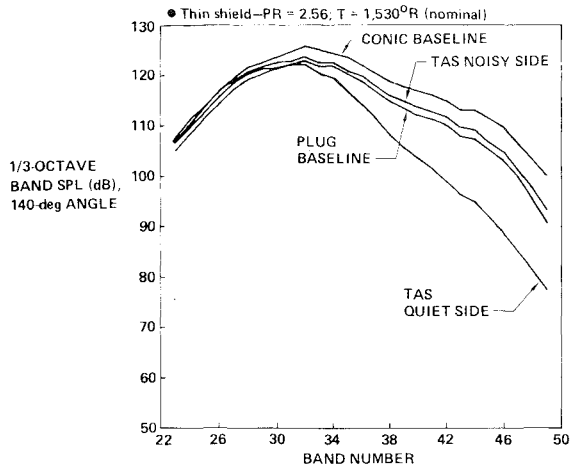

Fig. 19 Noisy-quiet side comparison, 140 deg.

The kind of result expected can be seen in Fig. 17 where results for the plug nozzle without the TAS are plotted. As expected, the greater mixing noise of the higher temperature results in more noise at equal pressure ratios. To date, no mechanism to explain why the TAS did not conform has been offered. These results do suggest that absolute temperature as well as temperature ratio is a controlling parameter in TAS performance.

Noisy Side vs Quiet Side

Noisy side vs quiet side measurements were also made. Comparisons are given in Fig. 18 for the 60 deg microphone and Fig. 19 for the 140 deg microphone. In these it can be seen that there is very little difference between plug baseline only and shield noisy side at the 60 deg angle. This suggests little if any reflection out of the jet in the forward direction. On the other hand, at 140 deg the noisy side is noisier than the plug only by approximately 2 dB, showing reflection to be one of the (but not the only) mechanisms of shielding.

Future Developments

A more comprehensive study than the tests reported here is in progress by the General Electric Company in Cincinnati, Ohio, under contract (NAS3-22137) from NASA Lewis Research Center. Several configurations are to be tested with a free jet to simulate relative velocity (flight) effects. Extensive instrumentation, a laser velocimeter, and theoretical

studies are expected to give additional insights into the mechanisms involved.

Conclusion

A thermal acoustic shield with a high-radius-ratio plug nozzle has demonstrated substantial noise suppression at intermediate jet velocities. However, suppression is considerably reduced at high jet velocities, with uncertainty as to the role of absolute jet temperature in this regime. The tests reported here indicate interactions with the jet shock structures that merit further study. They also show that with this configuration there is a sensitivity to shield nozzle location that affects the flow through the nozzle.

When the TAS is implemented with the shield obtained entirely by bleed from the main propulsive stream, the implicit thrust loss results in the noise reduction being small. It is expected however that results at the higher temperatures representative of an SST engine will show some improvement. Then, with optimization of thickness and velocity, the device could make such an engine competitive for noise with a coannular jet engine.

If a way can be found to implement the TAS in an additive mode without resizing the baseline engine, an impressive noise reduction could be obtained. The resulting incidental penalties (weight, drag, fuel burn, mechanical complexity, etc.) would then determine the overall effectiveness.

The big challenge is to implement a TAS with minimum performance loss so that the noise reduction potential can be realized. However, even the bleed system is worthy of work to explore and define its limitations further and to investigate it in combination with other suppression devices.

References

[1]Cowan, S.J. and Crouch, R.W., "Transmission of Sound Through a Two-Dimensional Shielding Jet," AIAA Paper 73-1002, Oct. 1973.

[2]Ahuja, K.K. and Dosanjh, D.S., "Heated Fluid Shroud as an Acoustic Shield for Noise Reduction—An Experimental Study," AIAA Paper 77-1286, Oct. 1977.

[3]Lu, H.Y., "Noise Attenuation by a Fluid Layer of Semi-Annular Cross Section," Boeing Doc. D6-42774, Dec. 1975.

[4]Goodykoontz, J., "Effect of a Semi-Annular Thermal Acoustic Shield on Jet Exhaust Noise," NASA TM-81615, Nov. 1980.

[5]McGehee, B.L., "A Test Facility for Aircraft Jet Noise Reduction," Paper presented at Institute of Environmental Sciences Annual Conference, April 1976.

[6]Peery, K.M. and Forester, C.K., "Numerical Simulation of Multi-Stream Nozzle Flows," AIAA Paper 79-1549, July 1979.

[7]Kowalski, E.J., Peery, K.M., and Klees, G.W., "Numerical Simulation for the Design of a Supersonic Cruise Nozzle with Fluid Noise Shield," AIAA Paper 81-1218, June 1981.